The Journal of Engine Research
Winter 2025, Vol. 71, No. 4, pp. 58-76
Journal Homepage: www.engineresearch.ir

Original Research

# Reduction of fuel consumption and emissions of Iranian naturally aspirated engine on Samand vehicle with thermal management

Arash Mohammadi[1]*, Yaghoub Montazer[2], Hossein Rahimi Asiabaraki[3]

[1] Faculty of Mechanical Engineering, Shahid Rajaee Teacher Training University, Tehran, Iran
[2] Iran Khodro Powertrain Company (IPCO), Tehran, Iran
[3] Department of Mechanical Engineering, National University of Skills (NUS), Tehran, Iran

**ARTICLE INFO**

***Keywords:***
Thermal Management
National Engine
Electric Thermostat
Electric Water Pump
Fuel Consumption

**ABSTRACT**

Reducing fuel consumption and greenhouse gas emissions in internal combustion engines is a key objective for automobile manufacturers. Employing advanced cooling systems is an effective solution to achieve this goal. In this study, the impact of coolant temperature on brake-specific fuel consumption (BSFC), HC, CO, and NOX emissions, as well as blowby, was first investigated experimentally at the most frequent operating point of the European driving cycle (2000 rpm, 2 bar brake mean effective pressure) in a naturally aspirated engine using an electric thermostat. Subsequently, the influence of an externally driven water pump's speed on fuel consumption was evaluated at the eleven most frequent operating points of the European driving cycle, with consideration given to the coolant temperature difference between the engine's inlet and outlet as a function of coolant flow rate. By determining the minimum required flow rate for each of these points, the optimal speed of the electric water pump was established, constrained by a maximum allowable temperature difference of 6°C between the engine's inlet and outlet. Additionally, the pre- and post-catalyst temperatures at these eleven operating points were compared for both mechanical and variable-speed water pumps. Finally, a simulation using GT-SUITE software, validated with experimental data, was conducted to analyze the performance, cooling system, and power transmission circuit of the Samand vehicle equipped with the domestic naturally aspirated engine under the European driving cycle. The results demonstrate that adopting a smart cooling system in place of a conventional mechanical cooling system reduces fuel consumption (in terms of $CO_2$ emissions) by 1.2%. Furthermore, HC and CO emissions decreased by 10% and 43%, respectively, while NOx emissions increased by 27%.



* Corresponding author
*E-mail address:* amohammadi@sru.ac.ir (A. Mohammadi)

Received 24 February 2025; Accepted 2 May 2025
E-ISSN: 2345-4121/ISSN: 1735-5214

**Cite this article:** Mohammadi A, Montazer Y, Rahimi Asiabaraki H. Reduction of fuel consumption and emissions of Iranian naturally aspirated engine on Samand vehicle with thermal management. The Journal of Engine Research. 2025 Feb 19;71(4):58-76. doi: 10.22034/ER.2025.2053701.1077

## 1- Introduction

As the automotive industry continues to prioritize sustainability and efficiency, reducing fuel consumption and emissions remains a primary concern for vehicle manufacturers. One innovative approach to addressing this challenge is the adoption of advanced thermal management systems to replace conventional cooling systems. By integrating these advanced technologies, vehicles can achieve significant improvements in both fuel efficiency and emission reduction [1].

During the combustion process in an SI engine, the burned gas temperature rises to approximately 2500K. The engine generates heat, part of it is absorbed by the coolant circulating through the cylinder head, piston, and cylinder. However, improper cooling can lead to high temperature gradients in the cylinder head, highlights the critical role of the cooling system in engine performance, efficiency, and emissions control.

Increasing heat loss from the burned fuel to the combustion chamber reduces output power and torque, while decreasing it raises cylinder wall temperatures, which can trigger knocking. Gas temperature during combustion also affects emissions. Additionally, friction—which is influenced by engine heat transfer—contributes to parasitic losses in the cooling system. The cylinder liner temperature further determines lubricating oil viscosity, and temperature gradients may cause bore distortion. A portion of mechanical energy is converted into power loss and dissipated through the cooling system.

Traditional automotive cooling systems consist of the engine, thermostat, an air-cooled radiator, and a centrifugal pump driven by the crankshaft belt. The thermostat typically comprises a temperature-sensitive wax element that regulates coolant flow to the radiator. As temperature rises, the wax liquefies, opening the thermostat and allowing coolant to circulate through the radiator, where it cools before returning to the engine to absorb heat. Upon engine shutdown, the coolant temperature drops, causing the wax to solidify and close the valve [1].

The thermostat's operating temperature depends on the wax element's properties, which activate at a predetermined coolant temperature. In contrast, modern map-controlled thermostats incorporate a small resistor into the wax element, enabling expansion at a secondary fixed-point temperature—particularly beneficial for flex-fuel vehicles. This system allows multiple temperature settings regulated by the engine ECU, adjustable based on fuel type, load conditions, and sensor feedback [2]. A schematic of the map-controlled thermostat is shown in Figure 1.

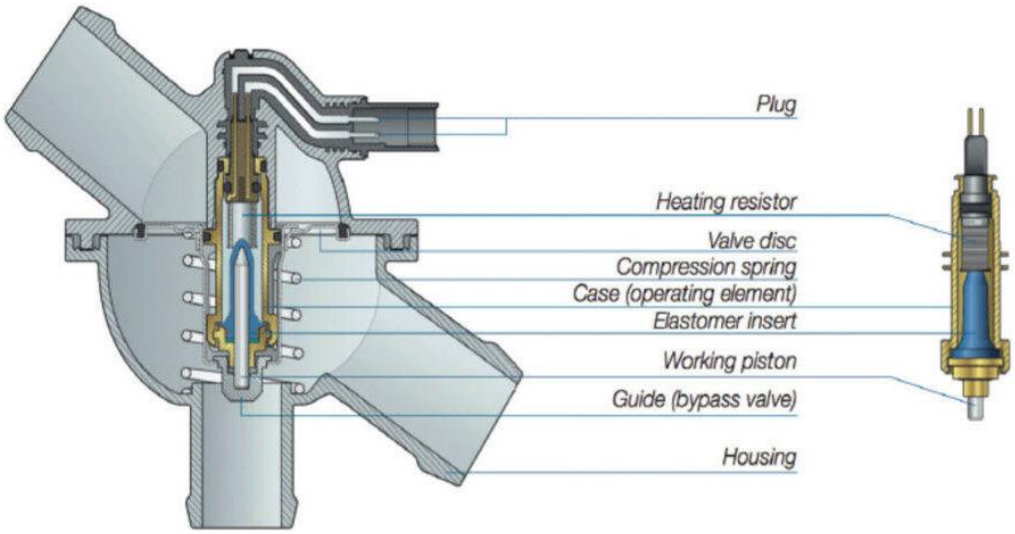


**Figure 1** Schematic of map-controlled thermostat

This leads to several positive effects:

1. Optimal combustion due to increased wall and component temperatures;
2. Reduced fuel consumption resulting from decreased viscosity of the engine oil and a corresponding reduction in frictional losses;
3. Lower emissions due to improved combustion;
4. Enhanced power output at full load owing to reduced coolant temperature;
5. Higher coolant temperatures and an improved interior heating and ventilation system [2].

On the other hand, conventional cooling systems utilize a mechanical water pump driven by a pulley with a constant ratio relative to engine speed. These systems are designed based on worst-case engine operating conditions (full load at all engine speeds), leading to excessive heat loss during part-load operation. To decouple the water pump speed from engine speed, a variable water pump can be employed. One approach in thermal management systems involves replacing the conventional mechanical pump with an electronically controllable electric pump. This modification can contribute to reducing emissions and improving brake-specific fuel consumption.

## 2- Literature Review

Extensive research has been conducted on the application of map-controlled thermostats. Guillemot et al. [3] demonstrated that the temperature of the cylinder head exerts a greater influence on HC emissions than that of the block. They also found that mixture preparation and blow-by in commercial gasoline engines are significantly improved by increasing the coolant temperature. Tomlinson et al. [4] described the capabilities of a map-controlled thermostat with PID closed-loop control for precise and stable operation. A parametric study was conducted through simulation to optimize engine performance.

Khanjani et al. [5] examined the feasibility of controlling coolant temperature across multiple drive cycles using an electric flow-control valve as a replacement for the conventional thermostat. The engine speed and load were used as inputs to a MATLAB Simulink model of the engine cooling system, incorporating an optimization algorithm. Consequently, a set of optimized coolant temperatures and corresponding brake-specific fuel consumption values were calculated. Their results demonstrated a reduction in fuel consumption of over 1% in urban and extra-urban cycles.

Fang et al. [6] investigated the effect of coolant temperature on performance and exhaust emissions (both gaseous and particulate) during the cold-start phase of a diesel engine. A simulated platform controlled the coolant pressure to replicate altitude conditions ranging from 0 m to 4500 m, with coolant temperatures varying between 20°C and 60°C. As the coolant temperature increased, CO and THC emissions decreased during the first 30 seconds of cold start. However, CO2 emissions remained relatively unaffected by changes in coolant temperature. Additionally, NOX emissions declined with higher coolant temperatures.

Bakatwar et al. [7] analyzed the performance of an engine cooling system equipped with an electronically controlled coolant thermostat to improve thermal efficiency. To integrate this technology with an IC engine, modifications were made to the thermostat housing geometry for mounting on the cylinder head. The ECU was programmed to regulate thermostat opening based on coolant temperature. The prototype system was evaluated in-vehicle to assess the impact of elevated coolant temperatures on engine performance. Results indicated significant improvements in thermal efficiency and exhaust emissions.

On the other hand, previous studies have investigated the use of variable-speed water pumps and the effects of coolant flow rate. In 2004, Jawad [8] simulated an engine cooling system with an electric water pump for vehicles and validated the model experimentally. The results demonstrated an increase in engine power output.

In 2005, Chalgren [9] analyzed a cooling system by substituting the mechanical water pump with an electric pump in a 5.7-liter diesel engine, achieving an 8% reduction in power losses.

In 2007, Chou [10] implemented a controllable electric water pump in a 4.6-liter six-cylinder diesel engine, showing that this replacement enabled a 27% reduction in radiator size.

Also in 2007, Michel [11] proposed a cooling system featuring a mathematical model of a controllable electromechanical actuator. This study maintained constant water pump and fan speeds while using an electric thermostat valve to regulate coolant temperature.

Ribeiro [12] demonstrated in 2007 that an electric water pump cooling system reduces fuel consumption, cylinder wall temperature, and emissions of NOx, CO, and HC.

In 2008, Turgut [13] performed experimental tests on a vehicle with a controllable thermal management system, evaluating factors such as full-load fuel consumption and coolant temperature.

Nasim [14] in 2012 conducted a simulation of a six-cylinder, four-stroke diesel engine using GT-Suite software to investigate warm-up time reduction through thermal management. By incorporating an electric pump and thermostat, they achieved a 200-second reduction in warm-up time and 3–9% improvement in specific fuel consumption compared to conventional systems.

In 2012 Santosh [15] developed a smart cooling system simulation for internal combustion engines using LabVIEW, controlling fan and water pump speeds based on coolant temperature. This approach yielded a 15% reduction in fuel consumption versus conventional cooling.

Iskander [16] in 2012 modeled a diesel engine cooling circuit with an electric water pump using GT-Suite, implementing a PID controller for pump speed regulation.

In 2013, Shin et al. [17] applied an electromagnetic clutch to a water pump, operating it in on-off mode to reduce warm-up time by 24.7% and fuel consumption by 4%.

That same year, Jung [18] in 2013 simulated a diesel engine cooling system with an electric water pump in AMESim, obtaining a 2.5% fuel consumption reduction and 21.3% shorter warm-up time (85 seconds faster than conventional systems).

In 2014, Arunachalam [19] reported a 3% fuel consumption reduction during warm-up after replacing a mechanical pump with an electric unit.

Tamim [20] in 2014 solved the coupled nonlinear equations of an engine cooling system, optimizing warm-up time via fuzzy control.

Masjoki et al. [21] in 2014 upgraded a cooling system by adopting an electric main pump. The electric pump's power demand (36–120 W) was significantly lower than mechanical pumps (800–1000 W), thereby reducing engine power losses.

In 2016, Mohammadi et al. [22] used GT-SUITE to simulate the cooling circuit of a naturally aspirated EF7 engine. By replacing the mechanical pump with an electric unit and developing a MATLAB Simulink fuzzy controller for speed regulation, they achieved a 39% reduction in warm-up time.

Despite these advancements, further research is needed to optimize coolant flow rate and temperature control strategies in naturally aspirated engines. This study addresses this gap by examining the combined effects of a variable-speed water pump and map-controlled thermostat on fuel consumption and emissions in an EF7 engine.

The research methodology comprised three phases:

1. Evaluation of coolant temperature's impact on fuel consumption, brake-specific fuel consumption (BSFC), and HC/NOx/CO emissions.
2. Analysis of coolant flow rate effects on BSFC and temperature differentials across the engine cooling jacket.
3. Simulation of a variable-speed water pump implementation in the EF7 engine using GT-SUITE software to quantify potential fuel and emissions reductions.

## 3- Methodology

First, to implement the map-controlled thermostat, the effects of coolant temperature (35–110°C) were experimentally investigated at 2000 rpm and 2 bar load (the most frequently repeated operating point in the NEDC cycle) on fuel consumption, brake-specific fuel consumption (BSFC), and HC, NOx, and CO emissions. The resulting data was used to program the thermostat to open at higher temperatures (110°C) under part-load conditions, while maintaining the conventional set point (90°C) for high-load operation.

Next, to determine the minimum allowable water pump speed (based on a maximum 6°C temperature difference between the inlet and outlet of the coolant jacket), the impact of coolant flow rate on BSFC and temperature differentials across the cooling jacket was analyzed. For these tests, eleven of the most frequent operating points in the NEDC cycle were selected (based on prior simulation experience) to identify the minimum permissible flow rate while adhering to the allowable temperature gradient. From these experimental results, a new water pump control map was derived.

Finally, to quantify potential reductions in fuel consumption and emissions, a variable-speed water pump was simulated on the EF7 naturally aspirated engine using GT-POWER software. By integrating the optimized coolant flow rates and temperatures as inputs for the variable-speed pump and map-controlled thermostat, a numerical model of the EF7 engine (as installed in the Samand vehicle) was developed in GT-POWER. This model was used to evaluate improvements in warm-up time and fuel consumption over the NEDC cycle.

### 3-1- Experimental setup for investigation of coolant temperature

The objective of this study is to analyze the effect of coolant temperature on the performance of naturally aspirated EF7 engines. To achieve this, experiments were conducted under controlled laboratory conditions. Figure 2 illustrates the test setup of the naturally aspirated engine in the laboratory environment. The coolant temperature was regulated through a heat exchanger and PID control system. A schematic diagram of all data acquisition systems used in this study is presented in Figure 3.

The fuel consumption was measured using a fuel monitoring system, while emissions were analyzed with an exhaust gas analyzer. The coolant temperature was varied between 35°C and 110°C. All tests were performed at a constant engine speed of 2000 rpm, 2 bar load, and λ=1. Once the coolant reached and stabilized at the target temperature, performance tests were conducted to measure fuel consumption and emissions. Engine specifications are presented in Table 1.

**Figure 2** Experimental setup in test room

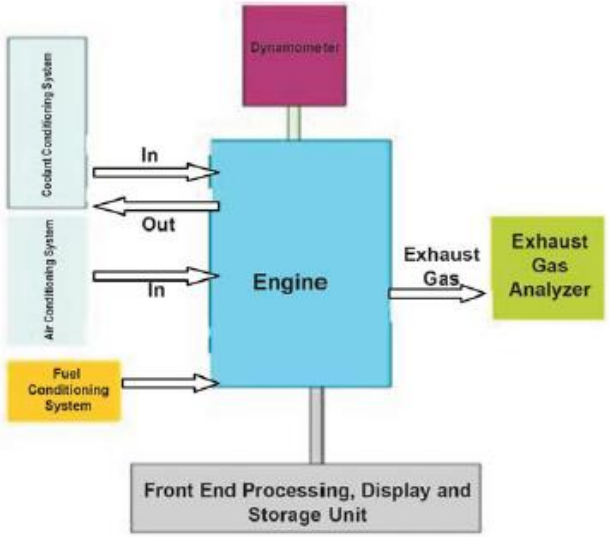


**Figure 3** Schematic experimental test-room

**Table 1** The engine specifications

| | |
|---|---|
| Bore | 78.6 mm |
| Stroke | 85 mm |
| Compression ratio | 11.5 |
| Connecting rod length | 133.5 mm |
| Displacement volume | 1646 cc |
| Fuel | Gasoline |
| Engine speed | 2000 rpm |
| Engine Load | 2 bar |

### 3-2- Experimental study of coolant flow rate of naturally aspirated on performance

The study examined a variable-speed water pump's impact on fuel consumption reduction using Iran's national naturally aspirated EF7 engine. Figure 4 illustrates the schematic diagram of the engine cooling system equipped with a mechanically-driven water pump powered by an external electric motor. As shown, the engine's coolant output splits into two pathways: one to the heater and another to the gas regulator. Two K-type thermocouples measure the coolant temperatures at the engine inlet ($T_{in}$) and outlet ($T_{out}$). These thermocouples, along with other laboratory instruments, enabled measurement of both coolant flow rate and emissions. All engine sensors were connected to a data logger interfaced with a computer for comprehensive monitoring.

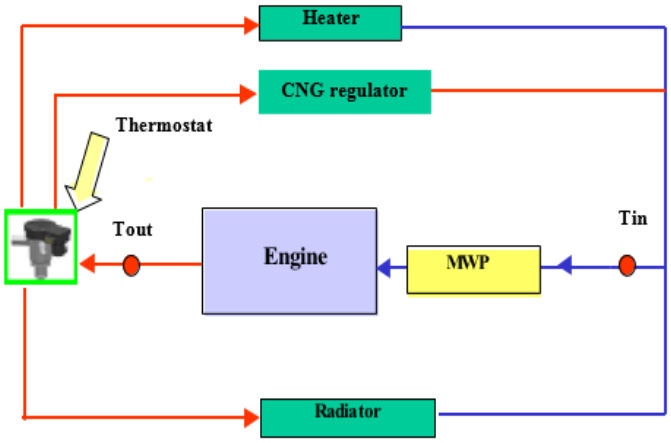


**Figure 4** Schematic of the EF7 engine cooling circuit

**3-3- Numerical model setup in GT-SUITE software**

The complete cooling circuit of a Samand vehicle equipped with a naturally aspirated EF7 engine was simulated using GT-SUITE software. As illustrated in Figure 5, the system comprises three primary components:

1. EF7 engine operating circuit
2. EF7 engine cooling circuit
3. Vehicle power transmission system

The simulation examined the cooling circuit in two configurations:

- Conventional cooling system
- Advanced system with map-controlled thermostat and variable-speed water pump

Key input parameters included:

- Performance characteristics of the water pump and thermostat
- Heat exchanger specifications
- HVAC system parameters
- Fan performance curves
- Oil cooler characteristics
- Pressure drops versus flow rate data for both radiator and heater

The hydraulic modeling approach divided the EF7 cooling system into:

1. Internal system (block and cylinder head cooling circuit)
2. External circuit (piping, radiator, fan, pump, thermostat, and heater)

This hydraulic modeling enabled determination of:

- Pressure distribution throughout the circuit
- Coolant flow rates in all system components

The simulation incorporated comprehensive engine specifications:

- Displacement volume
- Compression ratio
- Material properties
- Component dimensions
- Empirical test data (fuel consumption, friction losses, fan/pump performance) across various operating conditions

The cooling circuit modeling included detailed representation of:

- Internal coolant passages in the block and cylinder head
- Pipe network characteristics (diameters, lengths, materials, bend angles)
- Major components (radiator, pump, fan, thermostat)

The final simulation coupled engine performance with thermo-fluid analysis, tracking coolant flow:

1. Pump discharge into the engine block
2. Block cooling process
3. Flow transition to cylinder head
4. Final exit from cylinder head

For the power transmission system, input data included:

- Gearbox specifications
- Differential parameters
- Gearshift mechanism details

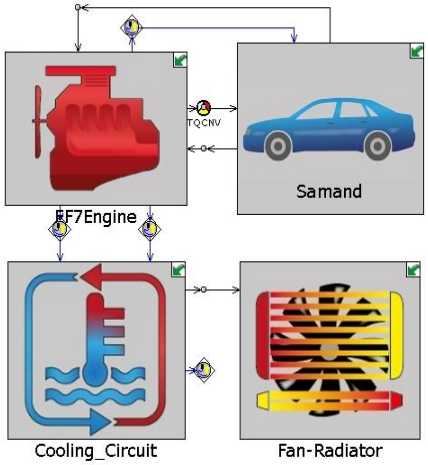


**Figure 5** Samand vehicle performance, cooling, and power transmission circuit

Figure 6 presents the standard operating and cooling circuit schematic for the EF7 engine. Following catalyst performance validation, the predetermined flow rates from Table 2 were implemented as control inputs for the variable-speed water pump. The power transmission circuit (Figure 7) models the complete drivetrain:

- Gearbox
- Differential
- Axles
- Wheels

All gear ratios (gearbox and differential) were input according to Samand vehicle specifications to ensure accurate simulation results.

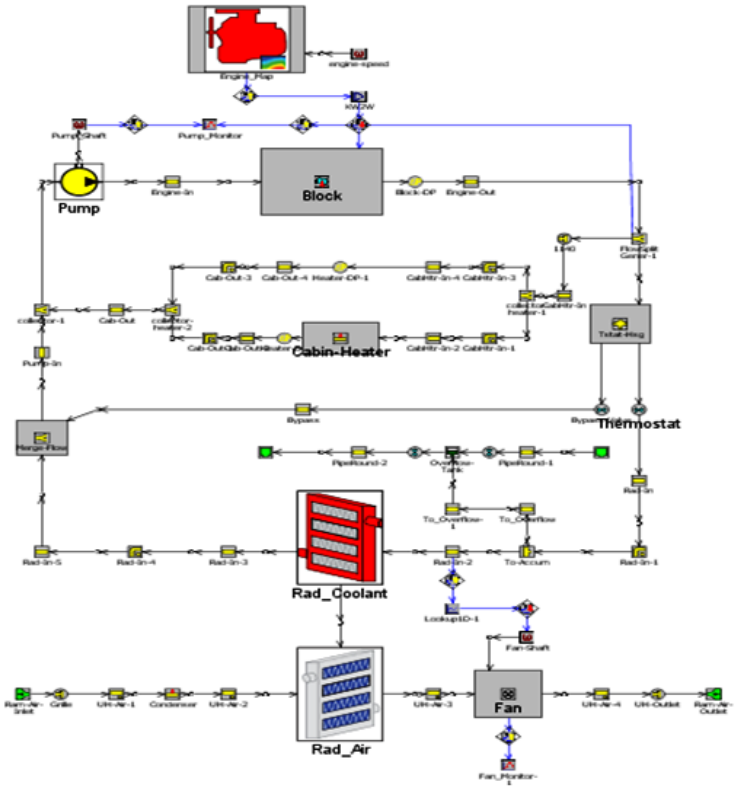


**Figure 6** Fluidic circuit simulation model of EF7 performance and cooling system

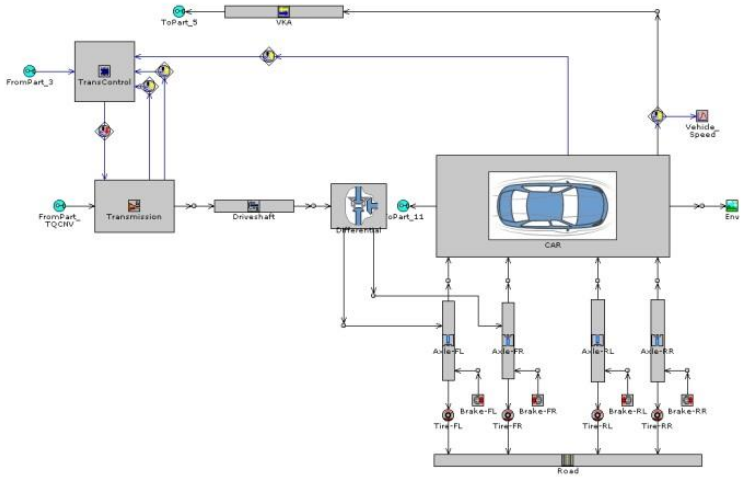


**Figure 7** Circuit simulation model of the Samand vehicle power transmission system

### 3-4- Governing Equations

The cooling circuit simulation was performed using GT-Cool, while engine performance was simulated with GT-Power, both within the Gamma Technology GT-Suite software environment. This 1D simulation platform models cooling system behavior under both transient and steady-state conditions. The numerical solution for fluid flow in the simulated circuit is obtained by solving the fundamental governing equations: continuity (Eq. 1), momentum (Eq. 2), and energy (Eq. 3).

$$\frac{\partial \rho}{\partial t} + \frac{\partial}{\partial x_k}(\rho u_k) = 0 \tag{1}$$

$$\rho\left(\frac{\partial u_j}{\partial t} + u_k \frac{\partial u_j}{\partial x_k}\right) = \frac{\partial \sigma_{ij}}{\partial x_i} + \rho f_i \tag{2}$$

$$\rho \frac{\partial e}{\partial t} + \rho u_k \frac{\partial e}{\partial x_k} = \sigma_{ij} \frac{\partial u_j}{\partial x_i} - \frac{\partial q_j}{\partial x_j} \tag{3}$$

For the coupled simulation of both performance and cooling circuits, heat transfer modeling must account for both conduction and convection mechanisms. The Fourier heat conduction equation (per unit area and time) can be expressed as:

$$\dot{q}_x = \frac{\dot{Q}}{A} = -k \frac{dT}{dx} \tag{4}$$

where k is the thermal conductivity. Heat is transferred by conduction from the inner surface of the block and cylinder head walls to the outer surface adjacent to the coolant. The amount of convection heat transfer is transferred by a fluid and a solid surface. The forced convection heat flux transferred to a solid surface with temperature $T_w$ by a fluid flow with average temperature T is calculated from equation (5).

$$\dot{q} = h_c\,(T - T_W) \tag{5}$$

where $h_c$ is the convection heat transfer coefficient, the value of which is calculated by the following equation:

$$\left(\frac{h_c L}{K}\right) = const. \times \left(\frac{\rho V L}{\mu}\right)^m \left(\frac{C_p \mu}{K}\right)^n \tag{6}$$

The constants $m$ and $n$ are empirical, determined experimentally based on the physics of the problem.

### 3-5- Numerical Methods

The integration accuracy (maximum relative error) for the Runge-Kutta solution algorithm determines the precision of numerical simulations. The relative error represents the difference between sixth-order and fifth-order Runge-Kutta solutions.

When this error exceeds the specified tolerance (ε), the time step is automatically reduced to maintain the desired accuracy level, ensuring consistent precision throughout simulations.

Users may adjust the accuracy parameter for two primary purposes:

- Computational Efficiency: Increasing ε (e.g., from 0.001 to 0.01) reduces simulation time when analyzing general trends where high precision is unnecessary.

- Solution Convergence: When anomalous results appear, decreasing ε helps verify whether they represent physical phenomena or numerical artifacts, thereby ensuring proper solution convergence.

This adaptive approach maintains an optimal balance between computational efficiency and solution accuracy while preserving numerical stability.

## 4- Results and Discussion

Figure 8 shows the fuel consumption and brake-specific fuel consumption (BSFC) of the engine as a function of coolant temperature at 2000 rpm and 2 bar load. The results demonstrate that both fuel consumption and BSFC decrease with increasing coolant temperature.

This trend can be attributed to reduced inducted air density in the combustion chamber at higher coolant temperatures, which increases the in-cylinder air temperature. Consequently, the engine control unit (ECU) maintains a constant air-fuel ratio (λ = 1) by reducing fuel injection, thereby lowering fuel consumption.

Additionally, the improvement in BSFC at higher coolant temperatures results from reduced heat loss to the cooling system, leading to better thermal efficiency. At lower coolant temperatures, more fuel is required to maintain the same brake mean effective pressure (BMEP= 2 bar), resulting in higher BSFC.

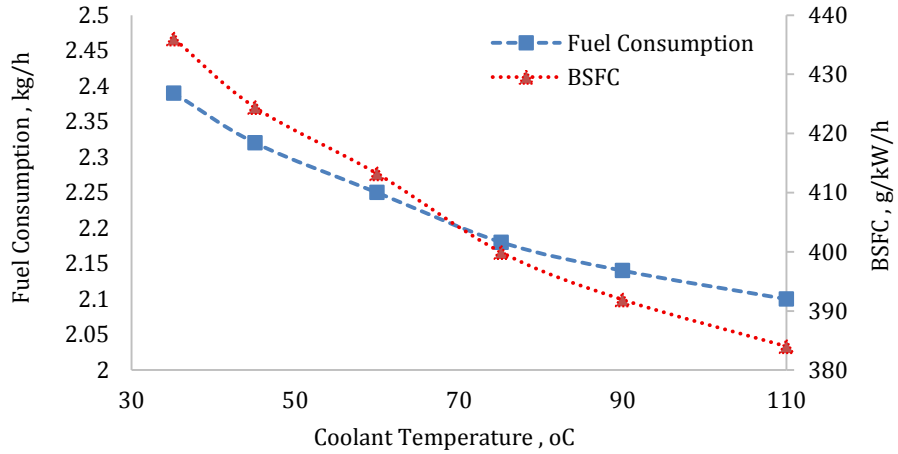


**Figure 8** Fuel consumption and BSFC for different coolant temperatures (2000 rpm, 2 bar)

Exhaust emissions were measured as a function of coolant temperature using an exhaust gas analyzer. Figure 9 presents the variations in unburned hydrocarbon (HC) and nitrogen oxides (NOx) emissions with coolant temperature at 2000 rpm and 2 bar load.

The results indicate that HC emissions decrease with increasing coolant temperature. This trend occurs because the cylinder wall temperature—which is directly influenced by coolant temperature—rises, promoting more complete fuel oxidation and reducing unburned HC formation.

Conversely, NOx emissions increase with higher coolant temperatures. In spark-ignition (SI) engines, NOx formation depends strongly on combustion temperature. As coolant temperature rises, the combustion chamber temperature increases, leading to greater thermal NOx production.

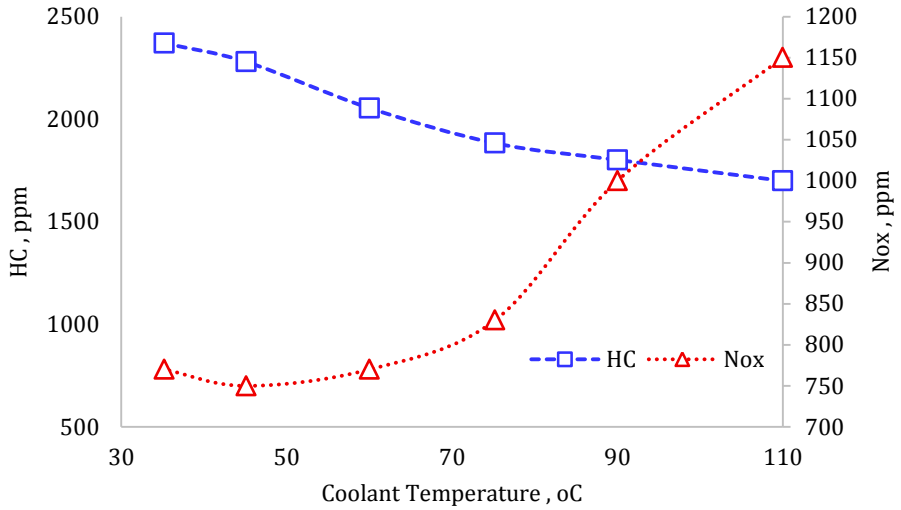


**Figure 9** unburned hydrocarbon and NOx for different coolant temperatures (2000 rpm, 2 bar)

Figure 10 shows carbon monoxide (CO) and Blowby versus coolant temperature. Carbon monoxide increases with rising coolant temperature. With increasing coolant temperature, combustion product temperature increases and more CO is generated during combustion.

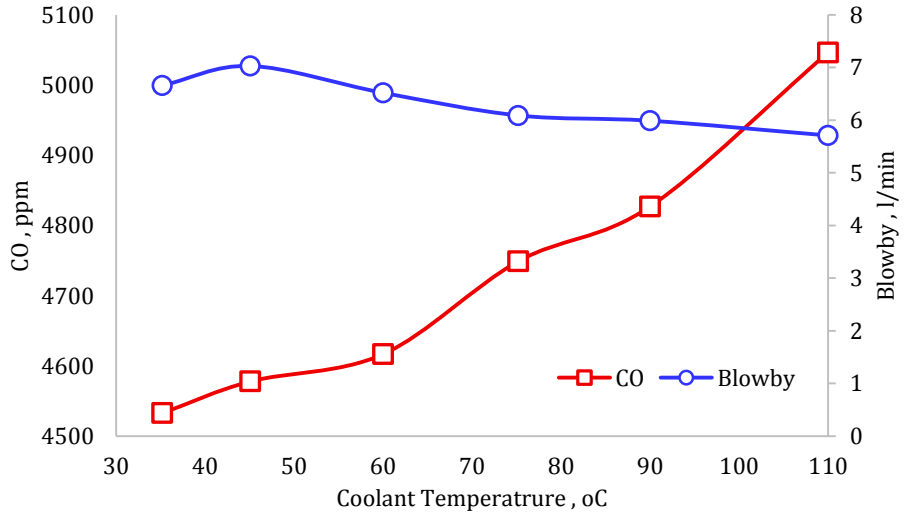


**Figure 10** Carbon monoxide and Blowby for different coolant temperatures (2000 rpm-2 bar)

**4-1- Experimental Results of coolant flow rate**

Figure 11 presents the test results of engine speed at full load conditions, showing the relationship between brake-specific fuel consumption (BSFC) and coolant flow rate for the mechanical water pump. The measured coolant flow rates ranged from 23.5 L/min at 1000 rpm to 142 L/min at 6000 rpm.

These flow rates are typically designed for worst-case operating conditions (full load), which differ significantly from the partial-load conditions encountered in the NEDC driving cycle. This presents an opportunity to reduce fuel consumption by optimizing coolant flow rates during NEDC operation. Lowering the coolant flow rate can improve engine output power and consequently decrease BSFC.

The critical consideration then becomes determining the minimum permissible coolant flow reduction that maintains adequate engine cooling while maximizing these efficiency gains.

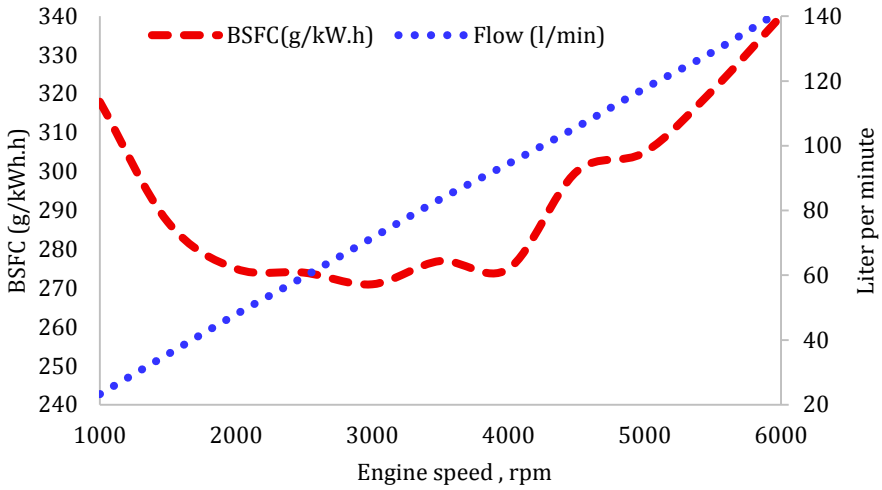


**Figure 11** Graph of brake specific fuel consumption and coolant flow rate at full load versus engine speed (Mechanical water pump)

To determine the minimum allowable coolant flow rate, the temperature difference between the engine's coolant inlet and outlet was measured, as shown in Figure 12. The results indicate a maximum temperature difference of 7.0°C at 1000 rpm and a minimum of 4.8°C. Accounting for experimental uncertainties, a conservative maximum temperature difference of 6°C was established as the threshold for determining minimum flow requirements. Exceeding this permissible temperature differential may lead to:

1. Excessive thermal gradients in the cylinder head
2. Elevated thermal stresses
3. Potential failure of the cylinder head gasket
4. Increased risk of engine knock

These constraints highlight the importance of maintaining proper coolant flow rates to ensure engine durability while optimizing fuel efficiency.

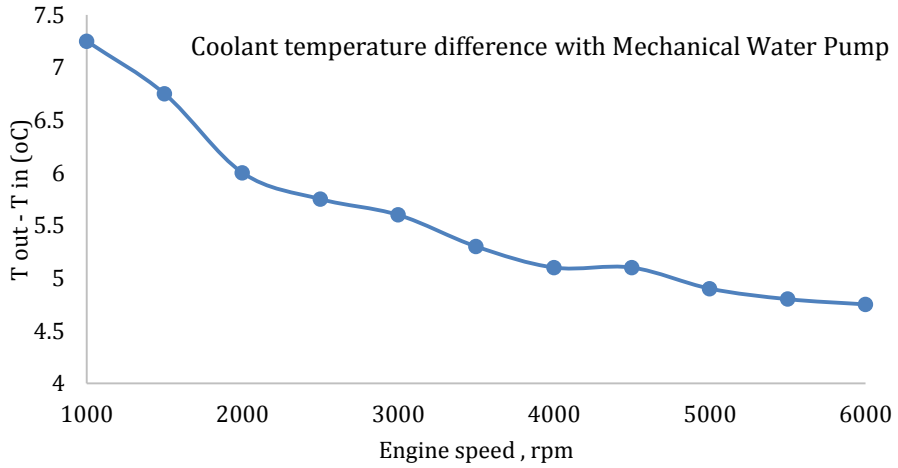


**Figure 12** Diagram of the difference in coolant temperature at the engine inlet and outlet versus engine speed

**4-2- Determining the flow rate of a variable speed water pump in eleven points of the NEDC cycle**

11 points that are most frequently repeated in the NEDC cycle (speed and load of engine), were considered according to Table 2 and then in every of this11 points, minimum water pump speed is determined.

**Table 2** 11 operating points of the EF7 engine in the NEDC cycle

| Speed (rpm) | BMEP (bar) |
|---|---|
| 834 | 0.403 |
| 915 | 2.46 |
| 1412 | 3.486 |
| 1857 | 1.39 |
| 2031 | 0.438 |
| 2047 | 4.338 |
| *2055* | 2.675 |
| 2439 | 0.972 |
| 2473 | 4.925 |
| 3099 | 3.498 |
| 3181 | 6.583 |

Figures 13 and 14 present the brake-specific fuel consumption (BSFC) and coolant temperature difference (between engine inlet and outlet) as functions of coolant flow rate for Cases 5 and 7 (referenced in Table 1). Similar trends were observed for the remaining test points.

Case 5 Analysis (Figure 13)

- Represents the 5th most frequent operating point in the NEDC cycle.
- A flow rate of 38 L/min was selected, maintaining a temperature difference of 5.5°C (below the 6°C threshold).
- At this flow rate, BSFC = 637 g/kWh, representing a 0.5% reduction compared to higher flow rates.
- No significant changes in temperature difference or BSFC were observed beyond 42–45 L/min.

Case 7 Analysis (Figure 14)

- Represents the 7th most frequent operating point in the NEDC cycle.
- A flow rate of 41 L/min was chosen, ensuring a 5.5°C temperature difference (within limits).
- Beyond 45–49 L/min, neither temperature difference nor BSFC exhibited notable variations.

Summary of Findings

- Table 3 compares the mechanical water pump's flow rates with the optimized values for an electric pump.
- The minimum permissible flow rates were determined based on 11 frequently occurring NEDC operating points, ensuring thermal safety (ΔT < 6°C) while maximizing fuel efficiency.

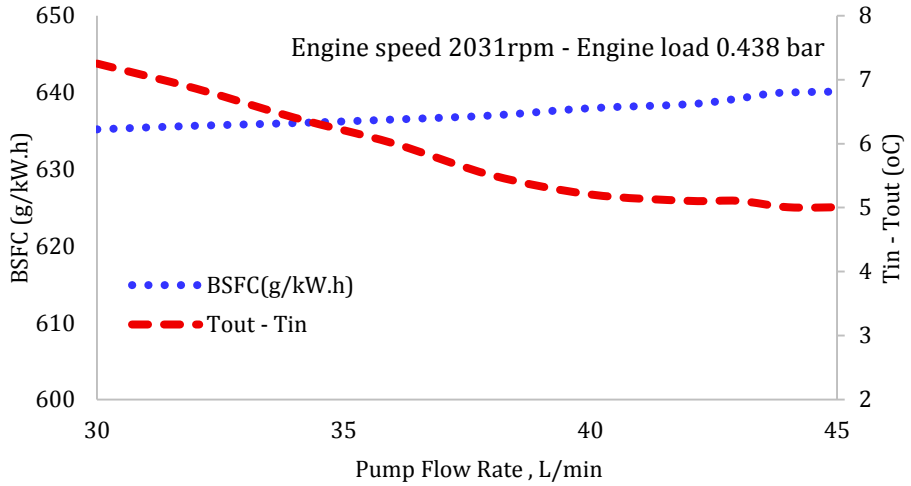


**Figure 13** Graph of brake specific fuel consumption and engine inlet and outlet coolant temperature difference versus engine coolant flow rate at 2031 rpm and 0.438 bar load

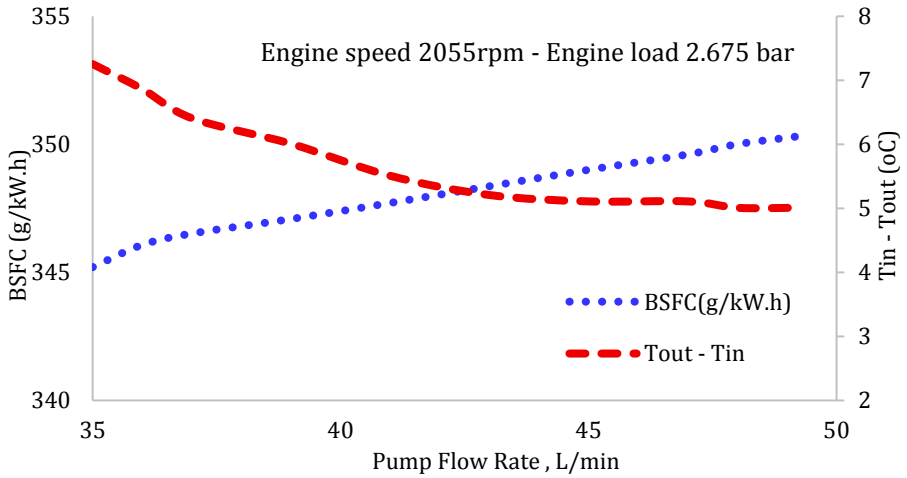


**Figure 14** Graph of brake specific fuel consumption and engine inlet and outlet coolant temperature difference versus engine coolant flow rate at 2055 rpm and 2.675 bar load

**Table 3** Estimated flow rates of variable speed water pumps compared to mechanical water pumps at eleven duty points of the NEDC cycle

| Speed (rpm) | BMEP (bar) | MWP (lit/min) | EWP (lit/min) |
|---|---|---|---|
| 834 | 0.403 | 19.0 | 10.0 |
| 915 | 2.46 | 21.2 | 12.01 |
| 1412 | 3.486 | 33.26 | 25.03 |
| 1857 | 1.39 | 45.02 | 36.0 |
| 2031 | 0.438 | 48.5 | 38.0 |
| 2047 | 4.338 | 49.1 | 43.0 |
| 2055 | 2.675 | 49.2 | 41.0 |
| 2439 | 0.972 | 58.0 | 50.0 |
| 2473 | 4.925 | 59.5 | 51.0 |
| 3099 | 3.498 | 72.0 | 62.0 |
| 3181 | 6.583 | 72.5 | 65.0 |

**4-3- Data analysis**

Tables 4 and 5 present pre-catalyst and post-catalyst temperature measurements using the optimized electric water pump flow rates (from Table 4). Key observations include:

1- Pre-Catalyst Temperatures (Table 4):

- Temperature differences between mechanical and electric pump configurations range from:
  - Minimum: 2°C (Item 6)
  - Maximum: 8°C (Items 1 and 5)
- The variable-speed pump increases pre-catalyst temperatures due to elevated cylinder gas temperatures
- This enables faster catalyst light-off compared to conventional pump operation

**Table 4** Temperature before the catalyst with mechanical and electric water pumps at eleven operating points of the European driving cycle

| Speed (rpm) | BMEP (bar) | MWP (°C) | EWP (°C) |
|---|---|---|---|
| 834 | 0.403 | 336 | 344 |
| 915 | 2.46 | 385 | 391 |
| 1412 | 3.486 | 451 | 455 |
| 1857 | 1.39 | 496 | 502 |
| 2031 | 0.438 | 470 | 478 |
| 2047 | 4.338 | 590 | 594 |
| 2055 | 2.675 | 520 | 527 |
| 2439 | 0.972 | 532 | 536 |
| 2473 | 4.925 | 674 | 678 |
| 3099 | 3.498 | 641 | 646 |
| 3181 | 6.583 | 742 | 746 |

2- Post-Catalyst Temperatures (Table 5):
- Temperature differences show:
  - Minimum: 3°C (Item 11)
  - Maximum: 10°C (Item 11)
- Higher exhaust gas temperatures with the electric pump similarly affect post-catalyst measurements

The data demonstrate that optimized coolant flow management:
- Enhances thermal conditions for catalytic converter activation
- Improves exhaust system heat retention throughout the aftertreatment process

**Table 5** Temperature after the catalyst with mechanical and electric water pumps at eleven operating points of the European driving cycle

| Speed (rpm) | BMEP (bar) | MWP (°C) | EWP (°C) |
|---|---|---|---|
| 834 | 0.403 | 370 | 379 |
| 915 | 2.46 | 426 | 432 |
| 1412 | 3.486 | 463 | 475 |
| 1857 | 1.39 | 496 | 503 |
| 2031 | 0.438 | 470 | 478 |
| 2047 | 4.338 | 592 | 602 |
| 2055 | 2.675 | 526 | 533 |
| 2439 | 0.972 | 524 | 529 |
| 2473 | 4.925 | 655 | 667 |
| 3099 | 3.498 | 646 | 655 |
| 3181 | 6.583 | 724 | 734 |

**4-4-Simulation Results**

Figure 15 compares the engine outlet coolant temperature profiles during the NEDC cycle for both conventional and variable-speed water pump configurations:

1. Conventional Mechanical Pump:
   - Pump speed correlates directly with crankshaft speed
   - Coolant temperature increases uniformly with a warm-up duration of 530 seconds
   - Temperature fluctuations after 530 seconds result from thermostat activation
2. Variable-Speed Electric Pump:
   - Pump remains inactive until coolant reaches 30°C
   - Rapid temperature rise occurs after 100 seconds (pump activation)
   - Temperature peaks then decreases to 77°C by 195 seconds
   - Thermal equilibrium with mechanical pump achieved at 326 seconds
   - Matching temperature profiles maintained through cycle completion

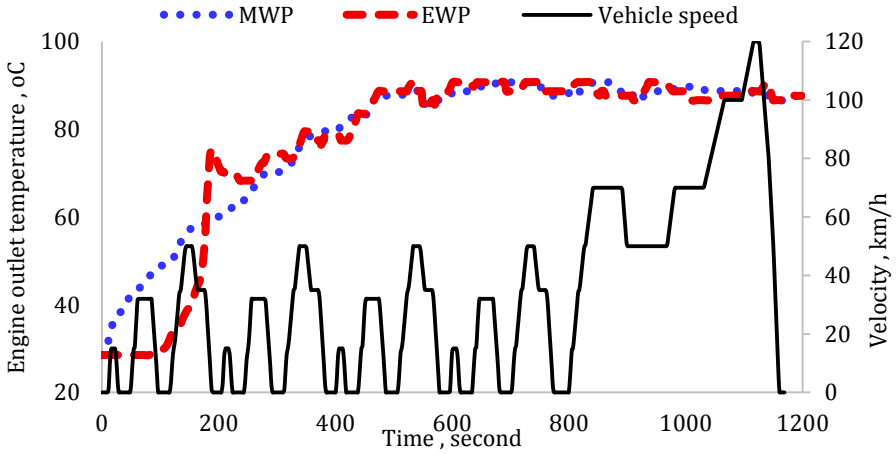


**Figure 15** Engine outlet fluid temperature diagram using an electric thermostat and electrical water pump in the European driving cycle

Key thermal management differences:

- Electric pump enables delayed activation for faster initial warm-up
- Achieves equivalent thermal stability 204 seconds sooner than mechanical system
- Maintains equivalent temperature control once stabilized

The data demonstrate the electric pump's advantages in:

1. Accelerated warm-up phase
2. Precise temperature modulation
3. Equivalent steady-state performance with reduced energy consumption

Figure 16 shows the graph of fuel consumption reduction in the NEDC cycle. The greatest reduction in fuel consumption (up to about 1.5 percent occurs after first 100 s. Because at the start of the vehicle's movement the coolant temperature is about 30 oC and the reduction in cooling improves combustion and increases the engine output. On average the reduction in fuel consumption is 1.2 percent.

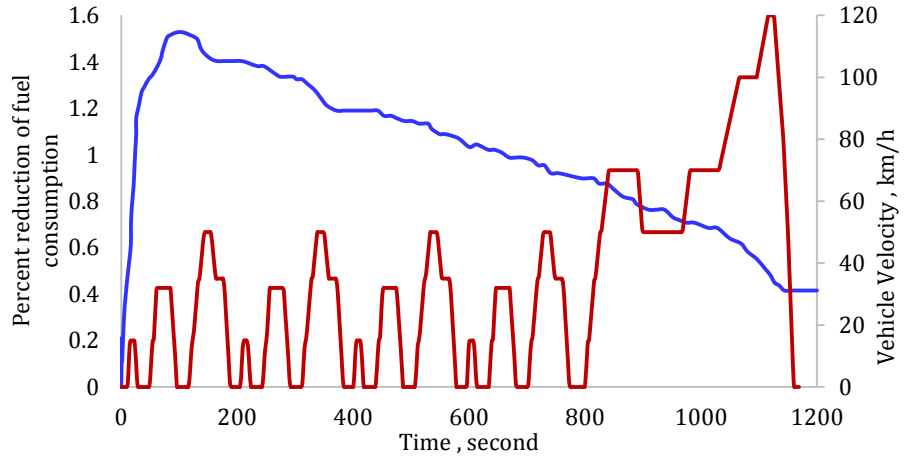


**Figure 16** Graph of fuel consumption reduction using an electric water pump in the European driving cycle (NEDC)

Emissions Testing Results (Tables 6 & 7):

The standardized emissions testing revealed significant differences between the variable-speed and conventional water pump systems:

1. Fuel Efficiency & $CO_2$ Reduction:
    - 1.2% decrease in fuel consumption
    - Corresponding reduction in $CO_2$ emissions
2. Hydrocarbon & Carbon Monoxide Emissions:
    - 43% reduction in HC emissions
    - 10% reduction in CO emissions
    - Primary causes:
        - Improved combustion efficiency
        - Reduced fuel consumption
3. Nitrogen Oxide Emissions:
    - 27% increase in NOx
    - Contributing factors:
        - Elevated combustion temperatures
        - Reduced heat rejection from engine cooling

Technical Interpretation: The variable-speed pump's thermal management strategy creates competing effects:

- Positive Impacts: Enhanced combustion quality reduces HC/CO through more complete oxidation
- Negative Trade-off: Higher cylinder temperatures promote thermal NOx formation via the Zeldovich mechanism

This analysis demonstrates the importance of balanced thermal management in achieving both emissions compliance and fuel efficiency targets.

**Table 6** Fuel consumption using an electrical thermostat and electrical water pump in the European driving cycle

| Description | Fuel Consumption (l/100KM) | CO2 (g/km) |
|---|---|---|
| MWP | 7.73 | 183.202 |
| EWP | 7.62 | 180.521 |
| Reduction percentage | 1.2% | 1.2% |

**Table 7** Emissions from electrical thermostat and electric water pumps in the European driving cycle

| Description | NOx (g/km) | CO (g/km) | HC (g/km) |
|---|---|---|---|
| MWP | 0.022 | 0.325 | 0.105 |
| EWP | 0.028 | 0.293 | 0.06 |
| Reduction percentage | -27% | 10% | 43% |

Fuel consumption in previous study [21, 22] is approximately 1-15. % that is in consistent we present study.

## 5- Conclusion

This research investigated fuel consumption and emissions reduction in the NEDC cycle by implementing a map-controlled thermostat and variable-speed water pump on the naturally aspirated EF7 engine (Samand vehicle). Key steps included:

- Identifying 11 high-frequency operating points in the NEDC cycle.
- Determining optimal coolant flow rates for the variable-speed pump while maintaining a permissible temperature differential (ΔT) across the engine.
- Evaluating the effects of coolant temperature modulation on emissions and efficiency.

Key Findings

1. Thermal Response Comparison
   - Conventional system: Gradual, uniform coolant temperature rise (~530 s warm-up).
   - Electric pump system: Rapid temperature increase after 100 s (delayed pump activation).
   - Post-warm-up: Both systems stabilize at comparable temperatures after ~250 s.
2. Catalyst Performance
   - Higher pre-/post-catalyst temperatures with the electric pump reduce light-off time, improving cold-start emissions control.
3. Fuel Efficiency
   - 1.2% reduction in fuel consumption (NEDC cycle).
   - Lower BSFC at elevated coolant temperatures due to reduced heat losses.
4. Emissions Trade-offs
   - Reductions:
     - HC: 43% (improved combustion efficiency).
     - CO: 10% (more complete oxidation).
   - Increase:
     - NOx: +27% (higher combustion temperatures from reduced cooling).

Technical Implications

The variable-speed system demonstrates:

- Faster thermal management during warm-up.
- Superior emissions control (HC/CO) but requires NOx mitigation strategies.
- Balanced efficiency gains without compromising engine reliability.

## References


[1] Thomas S, Saroop A, Rajak R, Muthiah S. Investigation on the effect of coolant temperature on the performance and emissions of naturally aspirated gasoline engine. SAE Technical Paper; 2011 Jan 19. doi: 10.4271/2011-26-0089

[2] Ribeiro EG, de Carvalho Meira JL, de Andrade Filho AP. Electric valve for coolant temperature control (TCV). SAE Technical Paper; 2007 Nov 28. doi: 10.4271/2007-01-2791

[3] Guillemot P, Gatellier B, Rouveirolles P. The influence of coolant temperature on unburned hydrocarbon emissions from spark ignition engine. SAE transactions. 1994 Jan 1:1237-47. doi: 10.4271/941962

[4] Tomlinson SP, Burrows CR. Design of a feedback controlled thermostat for a vehicle cooling system. SAE transactions. 1996 Jan 1:1677-83. doi: 10.4271/961823

[5] Khanjani K, Deng J, Ordys A. Controlling variable coolant temperature in internal combustion engines and its effects on fuel consumption. SAE Technical Paper; 2014 Nov 11. doi: 10.4271/2014-32-0064

[6] Fang L, Lou D, Hu Z, Tan P. The emission of a diesel engine in different coolant temperature during cold start at high altitude. SAE Technical Paper; 2019 Apr 2. doi: 10.4271/2019-01-0730

[7] Bakatwar R, Nesamani K, Bhargava A, Jain R. Performance analysis & optimization of engine cooling system by using electronically controlled thermostat for improving thermal efficiency. SAE Technical Paper; 2018 Apr 3. doi: 10.4271/2018-01-0053

[8] Jawad B, Zellner K, Riedel C. Small engine cooling and the electric water pump. SAE Technical Paper; 2004 Sep 27. doi: 10.4271/2004-32-0084

[9] Chalgren RD. Thermal comfort and engine warm-up optimization of a low-flow advanced thermal management system. SAE Technical Paper; 2004 Mar 8. doi: 10.4271/2004-01-0047

[10] Cho H, Jung D, Filipi ZS, Assanis DN, Vanderslice J, Bryzik W. Application of controllable electric coolant pump for fuel economy and cooling performance improvement. Journal of engineering for gas turbines and power. 2007;129(1):239-44. doi: 10.1115/1.2227035

[11] Mitchell T. Advanced thermal management for internal combustion engines [master's thesis]. Clemson: Clemson University; 2007.

[12] Ribeiro EG, de Andrade Filho AP, de Carvalho Meira JL. Electric water pump for engine cooling. SAE Technical Paper; 2007 Nov 28. doi: 10.4271/2007-01-2785

[13] Torregrosa AJ, Broatch A, Olmeda P, Romero C. Assessment of the influence of different cooling system configurations on engine warm-up, emissions and fuel consumption. International Journal of Automotive Technology. 2008 Aug;9:447-58. doi: 10.1007/s12239-008-0054-1

[14] Nessim W, Zhang F. Powertrain warm-up improvement using thermal management systems. International Journal of Scientific & Technology Research. 2012 May;1(4):151-5.

[15] Santhosh KV, Sharma NK. LabVIEW Implementation of an Automated Cooling Technique for Internal Combustion Engine using ANN. International Conference on Computing and Control Engineering (ICCCE 2012), 12 & 13 April, 2012.

[16] Iskandar MA, Adade Filho A. Design and analysis of a cooling control system of a diesel engine, to reduce emissions and fuel consumption. InABCM Symposium Series in Mechatronics 2012 (Vol. 5, pp. 39-48).

[17] Shin YH, Kim SC, Kim MS. Use of electromagnetic clutch water pumps in vehicle engine cooling systems to reduce fuel consumption. Energy. 2013 Aug 1;57:624-31. doi: 10.1016/j.energy.2013.04.073

[18] Jung D, Yong J, Choi H, Song H, Min K. Analysis of engine temperature and energy flow in diesel engine using engine thermal management. Journal of Mechanical science and Technology. 2013 Feb;27:583-92. doi: 10.1007/s12206-012-1235-4

[19] Arunachalam K, Jawahar PM. Conversion of Mechanical Water Pump to Electric Water Pump for a CI Engine. International Journal of Science and Technology. 2014;8(12):2087-90.

[20] Al-Tamimi A, Al-Jarrah AM, Salah MH. Inteligent Control Technoques for Electrical Actuated AAutomative Cooling Systems. Journal Control and Intelligent System. 2014;42(2).

[21] Shancita I, Masjuki HH, Kalam MA, Fattah IR, Rashed MM, Rashedul HK. A review on idling reduction strategies to improve fuel economy and reduce exhaust emissions of transport vehicles. Energy conversion and management. 2014 Dec 1;88:794-807. doi: 10.1016/j.enconman.2014.09.036

[22] Mohammadi K, Mohammadi A, Aghamirsalim SM. Simulation of cooling circuit with eletrical water pump in Iranian national engine with using Fuzzy controller. The Journal of Engine Research. 2022 Nov 27;44(44):19-30. [In Persian]

نشریه علمی تحقیقات موتور
زمستان ۱۴۰۳، جلد ۷۱، شماره ٤، صفحه ۵۸-۷۶
تارنمای نشریه: www.engineresearch.ir

مقاله پژوهشی

# کاهش مصرف سوخت و آلایندگی موتور ملی تنفس طبیعی روی خودرو سمند با استفاده از مدیریت حرارتی سامانه

آرش محمدی[۱*]، یعقوب منتظر[۲]، حسین رحیمی آسیابرکی[۳]

[۱] دانشکده مهندسی مکانیک، دانشگاه تربیت دبیر شهید رجایی، تهران، ایران
[۲] مرکز تحقیقات موتور ایران‌خودرو (ایپکو)، تهران، ایران
[۳] گروه مهندسی مکانیک، دانشگاه ملی مهارت، تهران، ایران

**اطلاعات مقاله**

**کلیدواژه‌ها:**
مدیریت حرارتی
موتور ملی
دمابان برقی
تلمبه آب برقی
مصرف سوخت

**چکیده**

کاهش مصرف سوخت و آلایندگی در موتورهای احتراق داخلی، یکی از مهم‌ترین اهداف برای تولیدکننده‌های خودرو است و در این راستا استفاده از سیستم‌های خنک‌کننده مدرن راه حل مهمی برای دستیابی به این هدف است. در این مقاله به‌منظور به‌کارگیری دمابان برقی ابتدا اثر دمای سیال عامل به‌صورت تجربی روی مصرف سوخت ویژه ترمزی، HC، CO، $NO_X$ و گازهای نشتی موتور در نقطه پرتکرار چرخه رانندگی اروپایی (سرعت ۲۰۰۰ دور در دقیقه و فشار مؤثر ترمزی ۲ بار)، در موتور ملی تنفس طبیعی بررسی شده است. در این مطالعه، تأثیر تغییر دور تلمبه آب بر مقدار شار سیال خنک‌کننده بررسی شده است. سپس، در یازده نقطه پرتکرار از چرخه رانندگی اروپایی، اثر این تغییر شار بر مصرف سوخت و همچنین اختلاف دمای سیال خنک‌کننده در ورودی و خروجی موتور اندازه‌گیری شده است. با مشخص شدن حداقل شار مجاز برای هریک از این یازده نقطه گانه، دور تلمبه آب برقی با بیشینه اختلاف دمای مجاز ۶ درجه تعیین می‌شود. همچنین دمای قبل و بعد واکنشگر در این ۱۱ نقطه کاری بین تلمبه آب مکانیکی و دور متغیر با هم مقایسه شده است. در نهایت با استفاده از نرم‌افزار GT-SUITE مدار عملکرد، خنک‌کاری و انتقال قدرت خودرو سمند با موتور ملی تنفس طبیعی چرخه رانندگی اروپایی بررسی شده است و مقدار مصرف سوخت و آلاینده‌های CO، $NO_x$ و HC در چرخه رانندگی اروپایی با خنک‌کاری معمول و خنک‌کاری هوشمند با هم مقایسه می‌شود. نتایج نشان می‌دهد با استفاده از سامانه خنک‌کاری هوشمند در مقایسه با سامانه مرسوم مکانیکی مصرف سوخت و $CO_2$ به ۱٫۲ درصد کاهش می‌یابد. همچنین HC به ۴۳ درصد، CO به ۱۰ درصد کاهش داشته اما $NO_x$ به ۲۷ درصد، افزایش می‌دهد.



* نویسنده مسئول
پست الکترونیکی: amohammadi@sru.ac.ir (آرش محمدی)

دریافت ۶ اسفند ۱۴۰۳؛ پذیرش ۱۲ اردیبهشت ۱۴۰۴
شاپای الکترونیکی: ۴۱۲۱-۲۳۴۵ / شاپای چاپی: ۵۲۱۴-۱۷۳۵

**Cite this article:** Mohammadi A, Montazer Y, Rahimi Asiabaraki H. Reduction of fuel consumption and emissions of Iranian naturally aspirated engine on Samand vehicle with thermal management. The Journal of Engine Research. 2025 Feb 19;71(4):58-76. doi: 10.22034/ER.2025.2053701.1077